Haptic Assistance for Helicopter Control based on Pilot Intent Estimation

Giulia D'Intino *
Max Planck Institute for Biological Cybernetics, 72076 Tübingen, Germany
University of Pisa, 56126 Pisa, Italy

Mario Olivari†, Heinrich H. Bülthoff‡
Max Planck Institute for Biological Cybernetics, 72076 Tübingen, Germany

Lorenzo Pollini§
University of Pisa, 56126 Pisa, Italy

Haptic support systems have been widely used for supporting human operators when performing a manual control task. These systems are commonly designed to track known target trajectories. However, the trajectory to track is not known in many realistic cases. For instance, the pilot intended trajectory is not known beforehand when considering a helicopter pilot flying in free-flight. This paper proposes a possible approach to design a haptic shared control system when the target trajectory is not known a priori. Especially, the aim of the proposed design is to help minimally-trained pilots during a 2-DoF lateral/longitudinal helicopter free-flight task. To accomplish this goal, first, a Pilot Intent Estimator (PIE) is developed to infer pilot intent. Then, the corresponding intended trajectory is generated. Finally, a haptic feedback is designed to track the estimated intended trajectory. The designed PIE was evaluated in a preliminary test with an experienced helicopter pilot. Then, a human-in-the-loop experiment with minimally-trained participants was conducted to assess the proposed shared control system. Results showed the effectiveness of the PIE to estimate the correct direction of motion chosen by the pilot. Furthermore, the haptic feedback helped participants to accomplish the control task with better task performance (i.e. lower tracking errors and lower amount of control activity) compared to manual control.

I. Introduction

NOWADAYS, automation is playing a key role especially in the autonomous driving and aviation fields. Automated systems are usually developed to ease the human operator effort to control a vehicle. Although partially or fully

*Ph.D Student, Max Planck Institute for Biological Cybernetics, 72076 Tübingen, Germany.
†PostDoc Researcher, Max Planck Institute for Biological Cybernetics, 72076 Tübingen, Germany.
‡Professor and Emeritus-Director, Max Planck Institute for Biological Cybernetics, 72076 Tübingen, Germany, Member AIAA.
§Associate Professor, Dipartimento di Ingegneria dell'Informazione, Faculty of Automation Engineering, 56126 Pisa, Italy Senior Member AIAA.

automated systems improve vehicles performance, they also reduce the operator situation awareness and increase risks due to wrong human-machine communication and interaction [1]. In particular, when the task of the human is to solely supervise the automation (i.e, human out-of-the-loop), problems like unbalanced operator mental workload and over-reliance on automation lead to skepticism and loss of operator skills [2, 3].

In the past few years, haptic systems have been proposed as a possible solution to enhance the human-machine relationship by means of tactile cueing. These systems allow the human operator to share the control with the automated system, thus increasing operator situation awareness [4]. Many studies are nowadays available on haptic support systems proving their effectiveness in terms of improved pilot performance and reduced workload [5, 6]. For instance, Mulder et al. designed a haptic gas pedal for a car-following task [7]. The pedal was developed to generate a continuous force signal to be shared with the force exerted by the driver. This helped the drivers to constantly be aware of the safe-field-of-travel and to avoid over-acceleration and over-deceleration that usually occur with manual control. In a different work, a haptic system was designed to assess pilot awareness when a failure occurs in a compensatory tracking task [8]. Pilot performance with haptic aid and with an automated system were compared before and after a failure of the system occurred. Results from a human-in-the-loop experiment demonstrated that the automated system was more effective for achieving better performance in the period before the failure. However, after the failure pilots could not achieve the same performance level as before. With haptic aid, instead, the pilots could get to the performance level before the failure.

In the aerospace field, use of haptic shared control systems as assistance systems for non-expert pilots is still poorly investigated. Mostly, these systems have been studied for learning purposes. Especially, haptic systems were evaluated to be effective for helping non-expert pilots to learn compensatory tracking tasks [9–11]. For instance, in a previous work a 2 degrees-of-freedom (DoF) haptic support system was developed to help inexperienced pilots to learn a compensatory tracking task in the pitch and roll axes [10]. The haptic aid was designed as a continuous force on the control device that was showing the right control strategy to the operator. Participants were trained either with or without haptic feedback in a human-in-the-loop experiment. Overall results showed that participants who trained with haptic aid learned the task faster compared to those who trained with manual control. In a different work, use of a variable haptic feedback was investigated for learning a disturbance rejection task in the roll axis, with difficult dynamics of the controlled element [11]. The haptic system was designed to variate in force and stiffness, in order to gradually give more control authority to the human operator. A human-in-the-loop experiment was performed to compare the designed variable haptic system to constant haptic feedback and to manual control. Participants were divided into three groups, according to the three conditions and trained in a fixed-base simulator. Results showed that the two groups, with variable and constant haptic aid respectively, learned the task faster compared to the manual control group. However, after the training, participants who trained with variable feedback were able to achieve better performance compared to the other groups. Use of a variable haptic aid was therefore shown to be more effective for learning a single-axis disturbance rejection task,

compared to constant haptic aid and to manual control.

Recently, human-machine interfaces based on haptic feedback were considered as a possible solution to help and support non-expert pilots during control of an aerial vehicle. Especially, these systems gained interest in the context of future aerial transportation with the aim of providing humans with aerial vehicles that may substitute cars and reduce congestion in the big cities. In this future scenario, the pilots would be required to receive only a minimum amount of training to learn how to control the vehicle, as the haptic system shares the control with the operator to support him. In a previous study on this topic, a easy-to-use control interface for personal aerial vehicles was designed based on haptic shared control [12]. Results from a human-in-the-loop experiment with non-expert pilots showed improved performance and lower pilot control activity and effort. In most of the previous works the haptic feedback was designed to track known target trajectories. However, predefined trajectories can be incongruous with the human operator intention, depending on the task that he/she is asked to accomplish. For instance, a haptic support system for lane-keeping was designed to track trajectories generated by a look-ahead algorithm that simulated human curve negotiation [13]. Although drivers achieved good performance with haptic aid, conflicts were occasionally generated due to a mismatch between the predefined trajectory and the driver intended trajectory. In a different work, a comparison between a direct and indirect haptic assistance (i.e, Direct Haptic Aid and Indirect Haptic Aid) was carried out to evaluate performance in a curve negotiation task [14]. Results from a human-in-the-loop experiment, conducted in a driving simulator, showed small disagreements between the two haptic controllers and the human operator during the task. Authors concluded that the disagreement was generated by controversies between the controller and the operator when cutting curves. Knowledge of the target trajectory is therefore essential to design a haptic feedback capable of helping operators to accomplish a manual control task.

In this paper, minimally-trained pilots are considered to fly a 2-DoF helicopter dynamics in a free-flight task. Control of a helicopter is a very difficult and demanding task for the pilot, due to its unstable and highly coupled dynamics. Haptic shared control may therefore be used to support the minimally-trained pilots to control the helicopter dynamics, while improving their performance and reducing the control effort in such demanding task. In a free-flight task however, pilots are free to choose any possible maneuver at any time. In contrast with the commonly studied manual control tasks, knowledge of the trajectory that the pilot intends to accomplish is not known to the system in advance in a free-flight task. In such case, estimation and prediction of the pilot intended trajectory is necessary for the design of the haptic feedback.

In shared control applications, prediction of future trajectories may affect the operators' behavior. Indeed, generation of trajectories that are different from the human intended trajectories may generate conflicts on the control device. These conflicts may lead to worse task performance and to critical situations during control of a vehicle. In a previous study, human operator's intended trajectory was estimated to reduce conflicts between the human and the haptic controller in a free-air movement teleoperation task [15]. To achieve this, a Gaussian Mixture Model algorithm was first trained to learn trajectories from operators demonstrations, then used to estimate the actual operator intended trajectory

when performing the task. Results from a human-in-the-loop experiment demonstrated that use of individualized trajectories for haptic shared control reduced conflicts between the human operator and the haptic system. However, this resulting haptic support produced poor results in situations different from those demonstrated during the learning process. In a different study, pilot intended trajectory was inferred to predict aircraft path to manage air-traffic in a future free-flight environment [16]. The trajectory was estimated based on aircraft state, weather and broadcast information (i.e, flight plan). However, when considering a helicopter free-flight control task, no prior knowledge of the flight plan or environmental constraint and limits are available. Only the actions made by the pilot on the control device can be considered to infer pilots intended trajectory. Therefore, estimation and prediction of those trajectories in the considered helicopter free-flight task represent a challenging problem.

In a recent work from the present authors, a Pilot Intent Estimator (PIE) was designed to estimate the pilot desired trajectory in a helicopter free-flight task according to pilot inputs [17]. The PIE was based on the Interacting Multiple Model filter (IMM) [18]. The IMM estimates the probability of a system to switch between different behavior modes (models) of the system itself. Four modes were defined to describe the helicopter dynamics: lateral, longitudinal, vertical and yaw motions. The proposed PIE was only validated in a simulation study with real pilot inputs recorded during a lateral reposition maneuver. Results showed that the PIE correctly inferred pilot intent. In a later work, the Pilot Intent Estimator mentioned above was used to generate the operator intended trajectory for a haptic support system [19]. Specifically, the PIE was designed to estimate pilot intent in a 2-DoF (Degrees of Freedom) control task with simplified dynamics of the controlled element, and a haptic aid was designed to track the estimated pilot intended trajectory. Results from a human-in-the-loop experiment showed that haptic feedback helped participants to accomplish the task with better performance in terms of tracking error, compared to manual control.

The goal of this paper is to design and experimentally evaluate a haptic shared control system as guidance assistance system for minimally-trained pilots involved in a more realistic task compared to the previous studies, i.e. 2-DoF lateral/longitudinal helicopter free-flight task. Due to the complex dynamics of the helicopter that makes control of this vehicle a highly demanding task for the human, the design of the proposed support system start from a simplified case: 2 degrees-of-freedom scenario with decoupled maneuver. The purpose of this paper is twofold. On the one hand, the paper aims at developing the algorithm to infer pilot intent according to his control actions, and to generate individualized trajectories for the haptic system. On the other hand, it aims at evaluating, with a human-in-the-loop experiment, the effectiveness of the haptic system designed to track the pilot intended trajectories, in order to help minimally-trained pilots to accomplish the task. The rationale of this work is to increase knowledge in the design of haptic shared control systems in the aerospace field, which is still poorly investigated. Especially, the contribution regards the design of the support system when no prior knowledge of the target trajectory is available to the system in advance.

The paper is structured as follows. Section II presents the design of the Pilot Intent Estimator and the haptic support system. Section III describes the design of the human-in-the-loop experiment conducted to evaluate the proposed

Table 1 Transfer functions of the dynamic model

Longitudinal axis	Lateral axis[a]
$\frac{\theta}{\delta_{lon}} = \frac{3.812(0.245)[0.226,14.758]}{(-0.438)(37.951)[0.792,0.869][0.1,14.335]}$	$\frac{\phi}{\delta_{lat}} = \frac{12.477(0.199)}{(-0.438)(37.951)[0.802,1.023]}$
$\frac{u}{\delta_{lon}} = \frac{2.465(-3.653)(3.631)}{(-0.438)(37.951)[0.792,0.8697]}$	$\frac{v}{\delta_{lat}} = \frac{-2.499(6.794)(-6.794)}{(-0.438)(37.951)[0.792,0.8697]}$

[a]Shorthand notation: $s + (1/T)$ is shown as $(1/T)$; $s^2 + 2\zeta\omega s + \omega^2$ is displayed as $[\zeta, \omega]$, where ω is the natural frequency and ζ is the damping factor.

system. Section IV presents results of a preliminary test phase conducted with an expert helicopter pilot. In Section V results from the final human-in-the-loop experiment are presented and are discussed in Section VI. The paper ends with conclusions.

II. Pilot Intent Estimation for Haptic System Design

Design of the haptic feedback is not trivial in a control task where no prior knowledge of the target trajectory can be assumed. This paper proposes a method to infer the pilot intended trajectory according to pilot inputs in a 2-DoF lateral/longitudinal helicopter free-flight control task. When no environmental constraints and cues are available to build a target trajectory (haptic lane keeping systems for motor-vehicles may resort to road boundaries to build pilot's intended trajectory for instance, but this is clearly not possible in helicopter free-flight), only the actions made by the pilot on the control device may give information about the trajectory that he/she intends to accomplish. Unfortunately, due to the coupled and unstable nature of the helicopter dynamics, the pilot actions necessary to produce the vehicle motion along one specific axis, are not limited to a clear motion of the stick along one direction: the pilot is constantly required to give a mixture of input commands in order to move the vehicle towards the desired direction, and, at the same time, to compensate for the cross-couplings and to stabilize the vehicle dynamics on both axis. Estimation of pilot intended trajectory in such case is therefore very complex.

The goal of this paper is to design a haptic system based on pilot intended trajectories to support minimally-trained helicopter pilots to accomplish their intended maneuvers. Inference of pilot intent is achieved through an estimation algorithm, which allows to distinguish between pilot inputs made to move towards a specific direction, and those inputs made to compensate for the cross-couplings, and/or to hover the helicopter. Then, pilot intended trajectories are generated to resemble the trajectories that an expert pilot would accomplish, when performing the same maneuver. This allows to help minimally-trained pilots to behave as an expert pilot. To achieve this goal, a probabilistic approach based on the Interacting Multiple Model is used to estimate the intended trajectory [18, 20]. Then, a haptic feedback is designed to help the pilot to track the estimated intended trajectory.

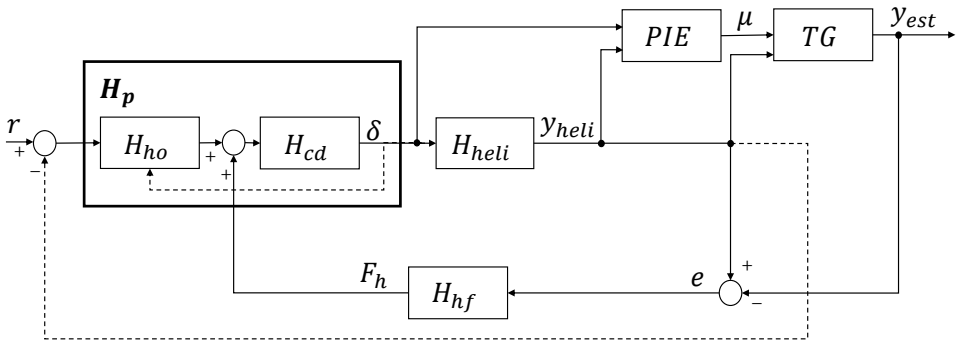

Fig. 1 Control scheme of the shared control system based on pilot intent estimation

Figure 1 shows the control scheme of the shared control system proposed in this paper. The block H_{heli} contains lateral and longitudinal decoupled dynamics of a Robinson R-44 helicopter model identified in hover condition [21]. Specifically, the dynamic model includes decoupled helicopter dynamics between inputs $\delta = [\delta_{lat}, \delta_{lon}]^T$ and outputs $y_{heli} = [u, v, \theta, \phi, x, y]^T$. The outputs vector takes into account longitudinal/lateral linear velocities u, v, attitude θ, ϕ and inertial position x, y. The considered transfer functions are shown in Table 1. The PIE block is the Pilot Intent Estimator designed to infer pilot intent. Specifically, this block estimates the probability μ of the intention of the pilot to produce a longitudinal only or lateral only motion. The block TG is the Trajectory Generator that computes the desired intended trajectory y_{est} along the estimated axis, according to the estimated probability μ. The block H_{hf} is the haptic feedback controller that generates the force F_h on the control device H_{cd} to help the human operator H_{ho} to track the intended trajectory, thus minimizing the tracking error e. H_p indicates the combined human operator-control device system. In the following, each block of the control scheme in Fig. 1 is described in detail.

A. Pilot Intent Estimator

The Pilot Intent Estimator (PIE) infers pilot intent according to pilot actions on the control device. The aim is to estimate which is the most probable direction towards which the pilot intends to move. The PIE was designed based on a probabilistic algorithm called Interacting Multiple Model filter (IMM) [20].

The IMM estimates the probability that a system matches one of several behavior modes (m_i models) that can be defined for the system itself. A general linear time-variant discrete time system can be described as:

$$x_k = A(k)x_{k-1} + B(k)u_k + w_{k-1} \tag{1}$$

$$y_k = C(k)x_k + v_k + D(k)u_k \tag{2}$$

with state vector x, input vector u, measurements y and process and measurements noise w and v. Matrices A, B, C, D

characterize actual system dynamics. A finite number of candidate modes m_i are defined as follows:

$$m_i : \{A_i, B_i, C_i, D_i\}, \quad m_i \in M \tag{3}$$

with A_i, B_i, C_i, D_i constant matrices representing a specific time invariant system dynamics, and M the set containing all the modes. Each mode m_i is employed as model dynamics in a Kalman Filter (KF) that estimates, at each time step, the expected state as output of the model according to pilot actions. Specifically, each i-th KF computes the state estimate and the evolution of the error covariance:

$$\hat{x}_{k_i} = A_i \hat{x}_{k-1_i} + B_i u_{k_i} \tag{4}$$

$$P_{k_i} = A_i P_{k-1_i} A_i^T + Q_i \tag{5}$$

and the corresponding estimate of the output as:

$$\hat{y}_{k_i} = C_i \hat{x}_{k_i} + D_i u_{k_i} \tag{6}$$

which lead to the residual:

$$r_{k_i} = y_k - \hat{y}_{k_i} \tag{7}$$

The residuals from each KF are used to asses which of the modes better match with the actual system dynamics. The comparison is carried out through a likelihood function. The likelihood values Λ_{k_i} are computed taking into account the residuals r_i, and indicate to which extent the actual system matches a mode m_i. Specifically, the likelihood values Λ_{k_i} are calculated as the normal distribution of the residuals with zero mean and residual covariance matrix S_i:

$$\Lambda_{k_i} = \frac{1}{\sqrt{2\pi |S_i|}} \exp(-\frac{1}{2} r_i^T S_i^{-1} r_i) \tag{8}$$

The probability that at time instant k a mode m_i is the correct mode(l)-match is given by:

$$\bar{c} = \sum_j p_{ji} \mu_{k-1_j} \tag{9}$$

$$\mu_{k_i} = \frac{\Lambda_{k_i} \bar{c}}{\sum_i \Lambda_{k_i} \bar{c}} \tag{10}$$

where p_{ji} is the probability to transition from a mode to another [18].

Figure 2 shows the block diagram of the Pilot Intent Estimator for a given mode m_i. The block $m_i - KF$ includes the equations of the Kalman Filter for the mode(l) m_i, the block $m_i - \Lambda_i$ computes the likelihood value Λ_i and the block

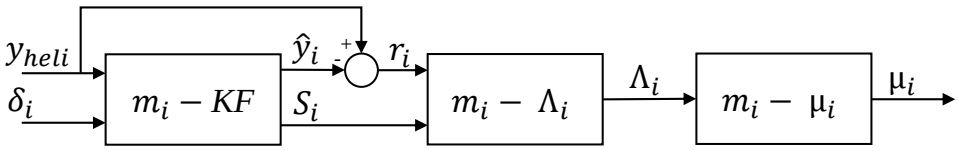

Fig. 2 Block scheme of the PIE for the i^{th} mode

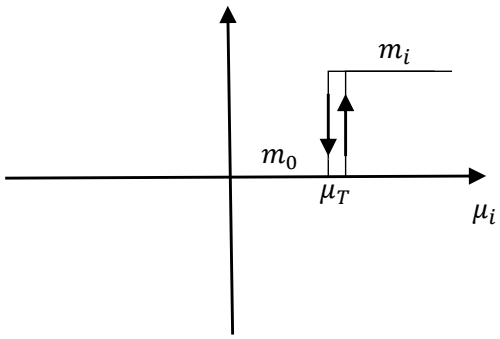

Fig. 3 Decider Function

$m_i - \mu_i$ computes the probability value of the mode m_i.

In this paper, the system dynamics was chosen as the 2-DoF (Degrees of Freedom) decoupled helicopter dynamics described in Table 1. Two modes m_1, m_2 were identified to describe the lateral and longitudinal behavior of the system. The first mode m_1 describes the helicopter dynamics with only the lateral input δ_{lat} acting on the system, and the second mode m_2 with the longitudinal input δ_{lon} active only. The pilot intention to move either in the lateral or in the longitudinal direction at time instant k is given by computing the probability μ_{k_i} in Eq. (10), where the values p_{ji} were set to 0.5 as the two modes have equal probabilities to be activated.

B. Trajectory Generator

The Pilot Intent Estimator provides the probability μ_i of the intention of the pilot to move either along the lateral or along the longitudinal axis. According to this estimation, a Trajectory Generator (TG) was designed to generate reference trajectories along the direction indicated by μ_i. Specifically, the direction of motion is selected by a Decider Function (DF), which implements a threshold function with hysteresis on μ_i. Figure 3 shows the Decider Function: the

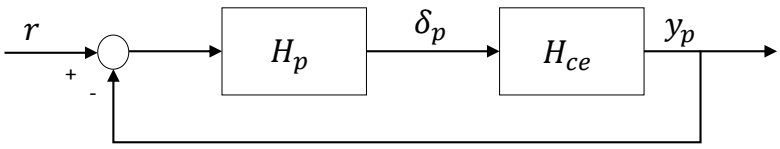

Fig. 4 Manual control schemes

mode m that is considered currently active is:

$$m = \begin{cases} m_1, & \text{if} \quad \mu_1 > \mu_T, \quad \text{lateral direction} \\ m_2, & \text{if} \quad \mu_2 > \mu_T, \quad \text{longitudinal direction} \\ m_0, & \text{if} \quad \mu_1, \mu_2 \leq \mu_T, \quad \text{hover} \end{cases} \tag{11}$$

The value μ_T is a threshold value and is chosen to be equal to:

$$\mu_T = p_0 + \epsilon \tag{12}$$

where $p_0 = 0.5$ corresponds to the probability of one of the two modes to be active, and $\epsilon = 0.05$ is a sensitivity offset whose value was found experimentally. Therefore, a mode m_i is activated when the corresponding probability μ_i is larger than the threshold value. A hover condition (i.e, mode m_0) is selected when none of the modes m_1, m_2 are activated. The hysteresis in the Decider Function accounts for oscillations in pilot inputs due to pilot errors, thus avoiding wrong activation of modes. With this approach, only one direction at a time is selected.

Given the estimated direction of motion, the intended trajectory y_{est} is generated as the trajectory that an expert pilot would accomplish when tracking the same reference as the actual pilot. Figure 4 shows the manual control scheme of a pilot H_p controlling a system dynamics H_{ce} and tracking a reference trajectory r, where the pilot dynamics block can represent both the dynamics of an expert pilot H_{pe} or that of a naive pilot H_{pn}.

The pilot intended trajectory y_{est} can be computed from the control scheme in Fig. 4, by using block diagram algebra. First, assuming that r is known, it is possible to compute the transfer function, for a naive pilot, from reference trajectory r to control inputs δ_{pn}:

$$H_1 = \frac{\delta_{pn}}{r} = \frac{H_{pn}}{1 + H_{ce}H_{pn}} \tag{13}$$

Then, the desired trajectory that an expert pilot would generate when tracking the same reference r is:

$$H_2 = \frac{y_{pe}}{r} = \frac{H_{pe}H_{ce}}{1 + H_{ce}H_{pe}} \tag{14}$$

The aim is to compute the transfer function between the trajectory of an expert pilot y_{pe} (i.e, desired y_{est}) given the inputs of a naive pilot δ_{pn}. Considering that the reference r is the same for both the naive and the expert pilot, the transfer function can be generated by combining the Eqs. (13) and (14):

$$H_3 = \frac{H_2}{H_1} = \frac{y_{pe}}{r}\frac{r}{\delta_{pn}} = \frac{y_{pe}}{\delta_{pn}} \tag{15}$$

Thus, obtaining the intended trajectory:

$$y_{pe} = \frac{H_{pe}H_{ce}}{1 + H_{ce}H_{pe}}\frac{1 + H_{ce}H_{pn}}{H_{pn}}\delta_{pn} \tag{16}$$

It follows from Eq. (16) that knowledge of the human pilot transfer functions H_{pe}, H_{pn} is crucial for generating a desired trajectory that resembles the trajectory of an expert human operator. A commonly used model of a human pilot involved in a manual control task is the McRuer's model [22]. Specifically, McRuer's theory assess that, in a manual control task, the human pilot adapts his control actions such that the open-loop dynamics between the pilot H_p and the system H_{ce} resemble a single integrator dynamics around the crossover frequency ω_c:

$$H_p H_{ce} = \frac{\omega_c e^{-s\tau}}{s} \tag{17}$$

Eq. (17) applies when considering a single DoF compensatory roll/pitch. In this work, the pilot control task is to track a trajectory along the longitudinal and lateral axes x/y while stabilizing the system dynamics. In such case, the human controller is supposed to give a compensatory feedback response on the attitude error, to stabilize the system, and a feedback response on the system outputs (i.e. velocity and position), to improve the tracking performance [23]. To account for these human responses, a triple-loop control was implemented to model both a naive and an expert pilot, and to obtain the corresponding transfer functions H_{pn}, H_{pe}.

Figure 5 show the implemented triple-loop schemes in the longitudinal and lateral axes (Figure 5a, 5b). Specifically, pilots are modeled by:

- inner loop: *attitude* loop H_{att} that accounts for control of pitch and roll errors (H_θ, H_ϕ);
- middle loop: *velocity* loop H_{vel} that accounts for longitudinal and lateral velocities (H_u, H_v);
- outer loop: *position* loop H_{pos} that accounts for longitudinal and lateral position (H_x, H_y).

The inner loop H_{att}, from the attitude error e_{att} to the inputs δ, was modelled according to McRuer's theory as in Eq. (17) [22]. Given the dynamics in Table 1, the transfer function H_{att} was described as:

$$H_{att} = H_p = K_p e^{-s\tau}(Ts + 1)\frac{1}{\frac{s^2}{\omega^2} + \frac{2\zeta s}{\omega} + 1} \tag{18}$$

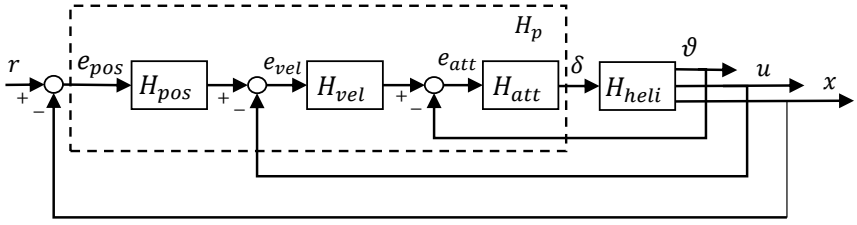

(a) Longitudinal axis.

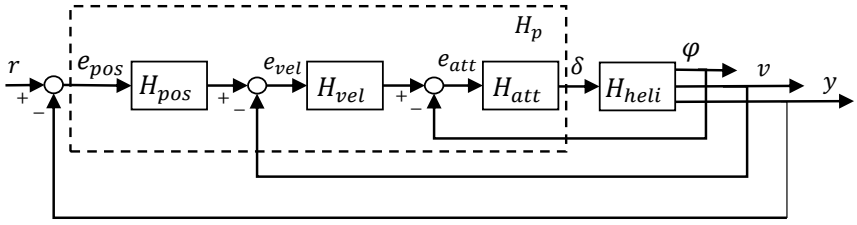

(b) Lateral axis.

Fig. 5 Open-loop transfer functions

where K_p is the pilot gain, τ is the visual delay, T is the time constant, and the complex conjugate poles represent the neuromuscolar dynamics. The visual delay was set to zero ($\tau = 0$), such that the desired trajectory y_{exp} is faster than the actual pilot trajectory y_{heli} (i.e, the obtained system is more responsive). The other parameters were set according to an identification process conducted with an experienced helicopter pilot involved in the control task, and are listed in Table 2.

The velocity loop (i.e, H_{vel}) was designed to stabilize the system dynamics. Specifically, the transfer function of the longitudinal axis H_u was chosen as:

$$H_u = \frac{K_u(T_{z_u}s + 1)}{(T_{p_u}s + 1)} \tag{19}$$

where K_u indicates the gain and T_{z_u}, T_{p_u} indicate the zero and pole respectively. The transfer function of the lateral velocity loop H_v was designed as a proportional controller:

$$H_v = K_v \tag{20}$$

The outer loop H_{pos} was designed to achieve a McRuer-like behavior such that the open-loop transfer function between H_p and the system H_{heli} acts as a single integrator around the crossover frequency ω_c, see Eq. (17).

Overall parameters of the designed triple-loop controller are listed in Table 2. Here, K indicates the gain, T_z, T_p indicate zeros and poles, and ω, ζ indicate the natural frequency and damping factor of the complex conjugate roots. Please note that Table 2 shows, for both lateral and longitudinal axes, the parameters obtained for the expert pilot only.

Table 2 Parameters of the lateral/longitudinal triple-loop transfer functions for an expert human pilot

Attitude Loop	K	T_z	ω	ζ
H_θ	-0.107	0.989	4.903	0.518
$H_\phi{}^a$	0.101	0.384	8.134	0.558
Velocity Loop	K	T_z	T_p	–
H_u	-0.07	0.002	0.599	-
H_v	0.189	-	-	-
Position Loop	K	T_z	T_p	–
H_x	0.04	100	8	-
H_y	0.0026	-	-	-

[a]Transfer function having all roots with multiplicity $m_r = 2$

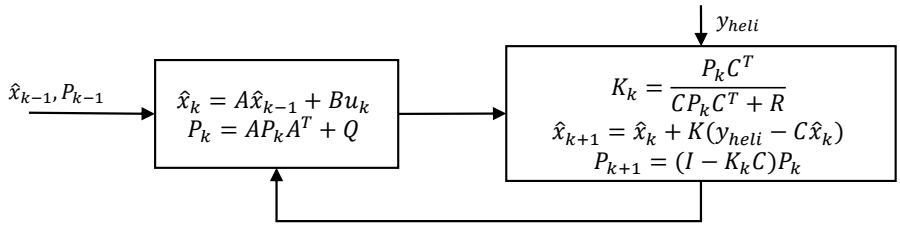

Fig. 6 Block scheme of the Kalman Filter algorithm

As described by McRuer's theory, the transfer function of a human operator in a manual control task is defined by the pilot gain, the lead-lag term and the pilot visual delay [22]. The parameter which influences most the closed-loop performance is the pilot gain, since it influences the open-loop gain, thus the bandwidth. Experimental evidence can be obtained to show that overall worse performance are achieved by reducing this parameter. In this work, the dynamics of a naive pilot is thus obtained by considering half of the value of pilot gain:

$$K_{pn} = \frac{K_{pe}}{2} \tag{21}$$

where K_{pe} indicates the expert pilot gain. Fig. 7 shows the bode plots of the open-loop transfer functions, in the longitudinal and lateral axes respectively, with the expert pilot transfer function drawn in black solid line, and the naive pilot transfer function drawn as a dashed line.

Finally, the computed transfer functions H_{pe}, H_{pn} are inserted in Eq. (16). Simple open-loop implementation of Eq. (16), due to the unstable nature of the helicopter dynamics, would surely lead to a divergence between the actual helicopter trajectory and the trajectory predicted by y_{pe}. Thus, with the goal of producing an intended trajectory that does not deviate excessively (or diverge) from the actual helicopter trajectory, the dynamics obtained in Eq. (16) was used as model for a Kalman Filter, that is fed with the actual helicopter trajectory y_{heli} as measurement for the estimated

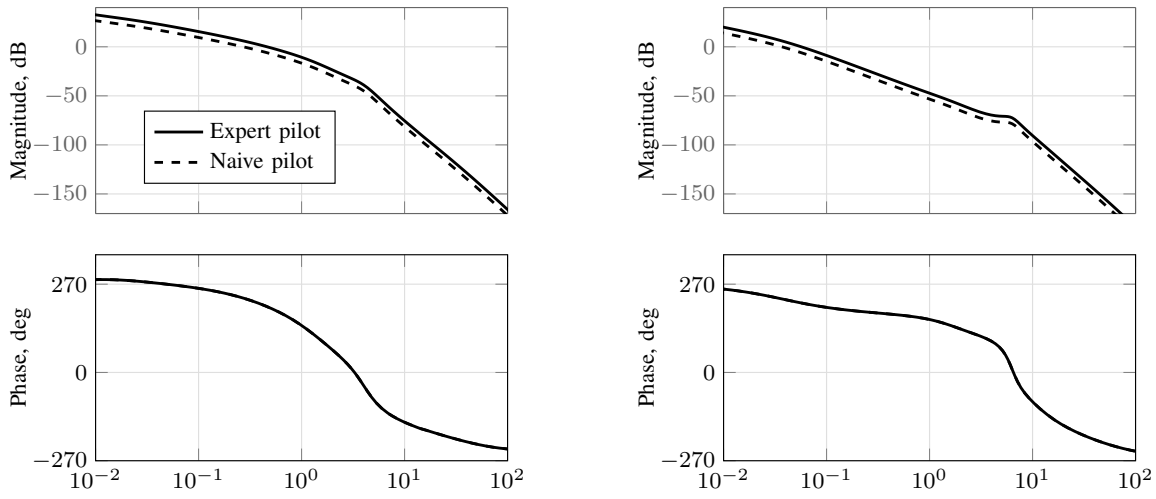

(a) Longitudinal axis. **(b) Lateral axis.**

Fig. 7 Open-loop transfer functions

y_{pe}. Figure 6 shows the structure of the Kalman filter in the Trajectory Generator block designed with the actual trajectory y_{heli} as measurement. The matrices A, B, C represent a state space realization of the dynamics in Eq. (16) and Q, R are the process and measurement covariances respectively. The use of a Kalman Filter allows the algorithm to predict stable trajectories, as it adjusts its estimation according to the actual measurements y_{heli} to converge to a stable prediction. The resulting predicted trajectory is the estimated pilot intended trajectory y_{est}.

C. Haptic Feedback

A haptic feedback was developed to help minimally-trained helicopter pilots to track the intended trajectory y_{est}, see Fig. 1. The haptic feedback was implemented as a force feedback on the control device. The force produced by the haptic system is shared with the human pilot on the control device and affects his/her control actions and may also generate conflicts [24, 25]. To overcome this issue, the haptic feedback was designed to mimic pilot actions, according to the crossover model [22]:

$$H_{hf} H_{cd} H_{heli} = \frac{\omega_c e^{-s\tau}}{s} \tag{22}$$

where H_{hf} is the haptic feedback and H_{cd} indicates the control device. Specifically, the haptic feedback was designed to resemble the dynamics of the expert pilot H_{pe} that was modelled with the triple-loop scheme in Fig. 5. Therefore, the dynamics of the haptic feedback is given by:

$$H_{hf} = \frac{H_{pe}}{H_{cd}} \tag{23}$$

With this approach, when the pilot is out-of-the-loop, the haptic feedback operates only to stabilize the helicopter dynamics. Instead, when the pilot is acting on the system, the haptic aid generates forces to track the estimated pilot intended trajectory.

(a) Fixed-base simulator.

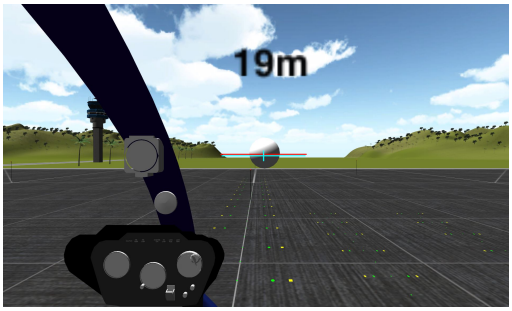

(b) Visual display.

Fig. 8 Experimental setup

III. Design of the Experiment

To validate the system in Fig. 1, first, a preliminary test was performed with one expert helicopter pilot, successively a human-in-the-loop experiment was conducted with minimally-trained participants. This section presents the design of the experiment. Please note that the same design was used for both the preliminary testing performed with one experienced helicopter pilot and the final experiment conducted with minimally-trained participants.

A. Experimental setup

The experiment was conducted at Max Planck Institute for Biological Cybernetics (Tübingen, Germany), using the fixed-base simulator shown in Fig. 8a. A control loading sidestick (Wittenstein Aerospace and Simulation, GmbH) was used as control device, and a high-resolution display (VIEWPixx, Inc.), with 120 Hz refresh rate, was used to show the visual environment to the human operator. The environment shown in Fig. 8b was designed in Unity®and included: the cockpit of an R-44 helicopter in a heliport, the artificial horizon and a gray sphere. The artificial horizon was realized with very minimal graphics: one horizontal line, one line aligned with helicopter body, and a central cross-mark. This cue was very useful to indicate the helicopter roll angle and to perceive the position of the sphere with respect to the helicopter center line, and therefore to visually estimate the lateral displacement with respect to the sphere. The sphere was used as moving target during the experiment and was at first located 20 m ahead of the helicopter. The target sphere was included in the design of the experiment as visual reference for the trajectory that the pilot had to follow to perform the experiment. This actually represents the ground truth of the pilot intended trajectory. Moreover, a numeric index was displayed on the upper part of the screen to show the distance between the helicopter and the sphere, in the longitudinal axis only. This information was important for the participant, in order not to get too close to the sphere. This would indeed degrade the participant's view of the environment, and therefore worsen the performance. In contrast, perception of the lateral distance was facilitated by the use of the artificial horizon, as described above.

B. Control task

The experiment task was to follow the target (i.e, the gray sphere in Fig. 8b), which was showing the maneuver to be accomplished. The maneuver that was chosen was inspired by the ADS-33, which includes a set of maneuvers that standard helicopters should accomplish [26]. Specifically, each trial lasted 90 s and the target was first moving along the longitudinal axis for 40 s, then holding position for 10 s and finally moving along the lateral axis for 40 s. These duration were chosen to better separate the two motions: longitudinal only and lateral only. Indeed, distinct motions produce clear results for the analysis. Moreover, due to the difficulties in perceiving the longitudinal distance to the sphere, the pilot was asked to maintain a distance from the sphere between 20 m and 15 m in the longitudinal axis in order to complete the task with best performance.

C. Experiment procedure

The experiment was divided into three phases: first, a familiarization phase was conducted to help participants understand the control task, successively each pilot performed 10 trials of the task with haptic aid and 10 trials with manual control. The last two phases were randomized between participants to avoid learning effects.

D. Independent variables

The experiment was influenced by only one factor: the presence of the haptic feedback. This feature is crucial to evaluate the effectiveness of the proposed system on participants performance, and to compare the results to the case in which no external aids are considered. This resulted in two experimental conditions.

E. Dependent variables

To evaluate differences in performance with and without haptic aid, two dependent variables (i.e. objective measures) were defined: the tracking error and the amount of pilot control activity. Specifically, the tracking error was chosen as metric for the tracking performance and was computed in terms of root means squared error, as following:

$$e_x = \begin{cases} 0, & \text{if} \quad 15 \leq d_x \leq 20 \\ \sqrt{\frac{\sum_{i=1}^{N}(d_x - 17.5)^2}{N}}, & \text{elsewhere} \end{cases} \tag{24}$$

$$e_y = \sqrt{\frac{\sum_{i=1}^{N} d_y^2}{N}} \tag{25}$$

where e_x and e_y indicate the tracking error in the longitudinal and lateral axis respectively. N is the total number of samples in one trial. The error is computed according to the distance d_x, d_y from the target sphere. Please note that, in the longitudinal axis x, the error is zero (i.e, best performance) when the pilot maintains a distance from the target between 15 m and 20 m in the longitudinal axis (see Eq. 24), while it is computed as the root mean square error of the

distance d_x when the pilot exceeds the defined boundaries. The two errors e_x and e_y are computed differently due to the design of the experiment: participants were asked to maintain the specified distance to the sphere along the longitudinal axis only.

A second measure considered for evaluation was the amount of control activity, which was used in previous works as an objective measure of the task workload [21, 27]. This measure was calculated as the amount of pilot inputs registered during each trial of the control task. To compute the measure, a dead-zone of amplitude δ_s, set to the 0.5% of the maximum stick deflection, was used: all input values δ below the threshold value δ_s were considered noise, and therefore were excluded from the measurement. According to this, the measurement accounts for inputs δ_{dz} that satisfy $\delta \leq -\delta_s$ or $\delta \geq \delta_s$. Therefore, the amount of control activity was calculated as:

$$W = \frac{\int \delta_{dz}}{T} \tag{26}$$

where δ_{dz} is the stick deflection pre-filtered by the dead-zone, and T is the overall time per each trial. As acknowledged in a previous work, this objective measure does not take into account all aspects of pilot's workload (e.g. pilot's cognitive process) [27]. In this paper, the measure in Eq. 26 was calculated to evaluate and compare pilots control strategy with and without haptic feedback. Specifically, with the help of the haptic system lower values of control activity would indicate that the pilot needed fewer control actions to accomplish the task. This would suggest that a different (i.e. less demanding) control strategy was adopted by the pilot with haptic feedback, compared to the case with no external aid.

IV. Preliminary Testing and Validation

A preliminary study was conducted with one expert helicopter pilot. The rationale was to investigate whether the designed haptic shared control system could help an expert pilot to accomplish the maneuver, without counteracting him during control of the system. For the testing, a civil helicopter pilot, licensed to fly light-weight helicopters (R-22, R-44), was considered. He had no previous experience with haptic feedback systems. Results of the preliminary testing were used as preliminary assessment of the system, for performing the final actual experiment with minimally-trained participants. As the purpose of this work did not include evaluation of the proposed system on expert pilots, only one pilot was considered in the preliminary testing.

The pilot performed first 5 trials of the control task with no external aid (i.e, manual control). This initial phase was used to validate the PIE. Successively, the expert pilot performed 20 trials of the control task, as in Section III.C: 10 trials in manual control and 10 trials with the haptic aid switched on. In this case a comparison between pilot performance with and without haptic feedback was used to evaluate the haptic shared control system.

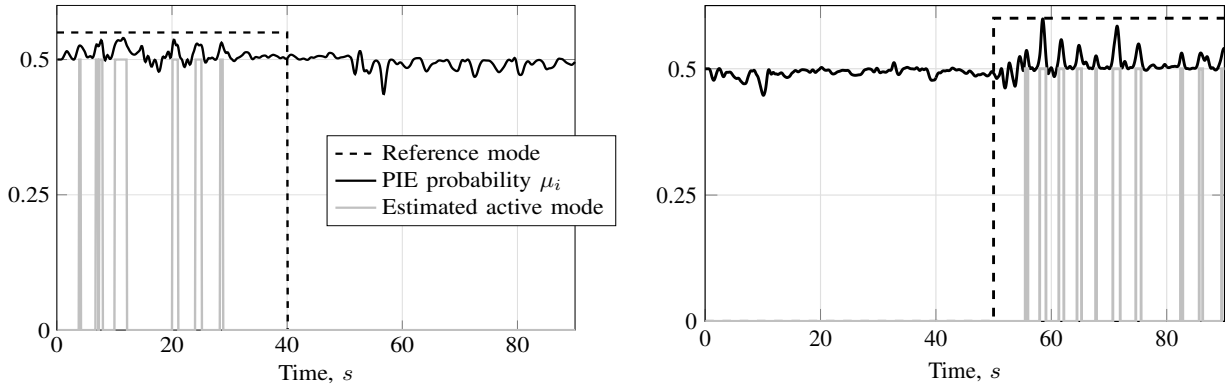

(a) Longitudinal motion. **(b) Lateral motion.**

Fig. 9 PIE estimated probability and mode selection during one trial

A. Hypotheses

Two main hypotheses were defined. The first hypothesis regards the Pilot Intent Estimator. Specifically, the PIE was supposed to correctly estimate the probability that the pilot was using one of the two control axes δ. Therefore, the probability μ_i was expected to become larger than the threshold value μ_T (see Fig. 3), when the target sphere moved along the corresponding direction. Furthermore, the Trajectory Generator was hypothesized to generate a good estimate of the trajectory that the pilot intended to accomplish along the axis corresponding to the mode estimated by the PIE.

The second main hypothesis considers the entire system with haptic feedback. Specifically, the haptic aid was expected to help the expert pilot to perform the control task. Therefore, the tracking error of the trials with haptic aid was hypothesized to have similar or lower values compared to the error achieved with manual control. Moreover, the task workload was expected to be reduced with haptic aid. Therefore, the pilot was supposed to put less effort to control the system dynamics with the help of the haptic system compared to manual control.

B. Preliminary results

This section presents the results of the preliminary study conducted with an expert helicopter pilot. An analysis of the estimated probability μ_i, the estimated active mode and the reference mode (assumed from the target motion), was conducted to validate the PIE. Moreover, in order to asses the effectiveness of the Trajectory Generator, the corresponding estimated trajectories are compared to the actual trajectories accomplished by the pilot during one trial of the control task with manual control. Successively, the overall system with haptic feedback is evaluated.

1. Validation of the Pilot Intent Estimator and Trajectory Generator

Fig. 9 shows the probability estimated by the PIE and the corresponding activated mode during one trial. Specifically, the estimated probabilities μ_i are shown in solid black line, the modes activated by the Decider Function are shown in grey and the mode corresponding to the target motion is shown as a dashed line. Fig. 9a shows the mode selection

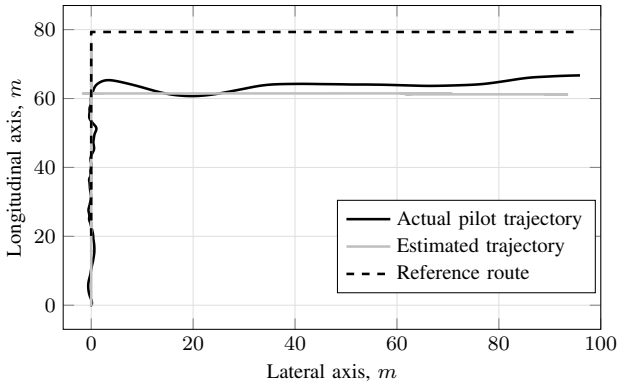

Fig. 10 Comparison between estimated trajectory and actual trajectory during one trial

during the longitudinal motion. The estimated probability μ_2 becomes larger than the threshold value μ_T during the maneuver (i.e, first 40 s of the trial). Therefore, the corresponding mode m_2 is activated by the Decider Function (grey plot). The activated mode corresponds to the mode activated by the target (dashed line), thus no wrong activation of modes occurred. At $t = 50$ s the target starts moving along the lateral axis, see Fig. 9b. To follow the target, the pilot activates the lateral mode m_1. Therefore, the estimated probability μ_1 increases and the corresponding mode is selected (in grey). During the hover condition (i.e, between 40 s and 50 s) none of the modes is activated by the Decider Function, thus mode m_0 is selected. The important aspect to be noticed in this figure, is the effectiveness of the algorithm in estimating the correct pilot's intended direction of motion, during both movements. During the first and the last 40 seconds, when a clear direction should have been detected, the algorithm recognized some portions of the movement as hover conditions: these are likely those moments when the pilot gave inputs to compensate for the cross-couplings or corrected his commands. Indeed, Figures 9a and 9b show that the probability of longitudinal motion is much higher than that of lateral motion in the first 40 seconds, while the converse happens in the last 40 seconds. Although the probabilities do not pass the thresholds, and thus do not activate the corresponding modes, during the entire duration of each motion, this result suggests that the PIE correctly distinguished between the two main directions of motion intended by the pilot, and recognized cross-coupling compensations and hover conditions, and more important, avoided wrong activation of modes which would have generated wrong target trajectories, resulting then in wrong haptic aid generation.

The trajectories corresponding to the PIE estimated probabilities are shown in Fig. 10. Specifically, the pilot actual trajectory is drawn in black, the trajectory generated by the Trajectory Generator block is drawn in grey and the target trajectory is shown in black dashed line. The target was located 20 m ahead of the helicopter and the pilot goal was to control the helicopter to follow the target while staying within 15 m and 20 m from it. As can be seen, the pilot intended trajectory is correctly generated along the axis corresponding to the activated mode.

In order to evaluate the effectiveness of the haptic feedback a comparison between pilot performance with and

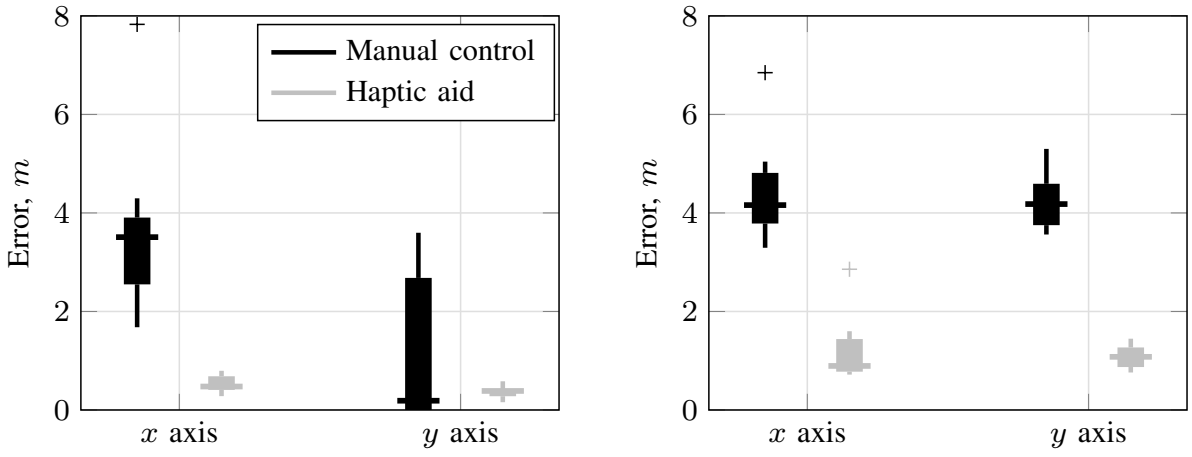

(a) Longitudinal motion. **(b) Lateral motion.**

Fig. 11 Preliminary results: boxplots of the tracking error overall the trials

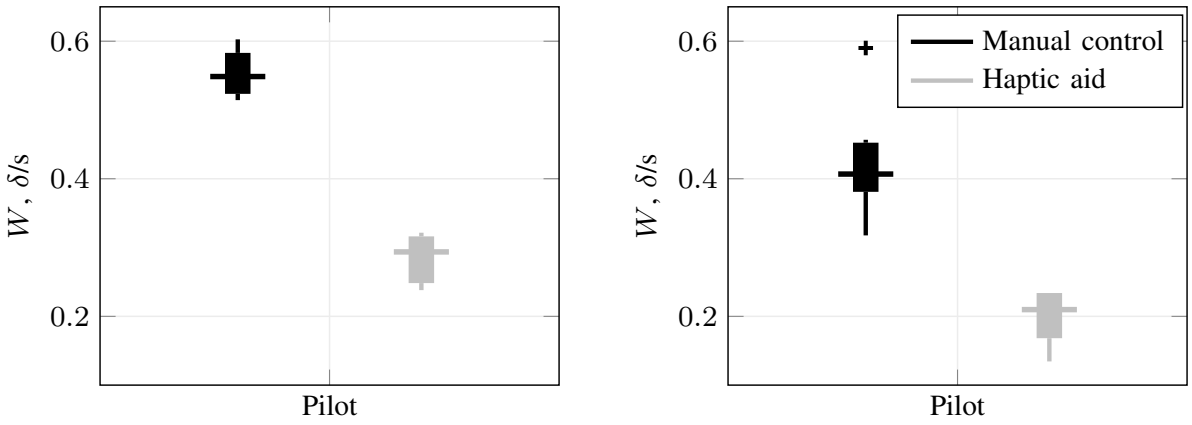

(a) Longitudinal motion. **(b) Lateral motion.**

Fig. 12 Preliminary results: boxplots of the task workload overall the trials

without haptic aid was carried out. Figure 11 shows the boxplots of the tracking error in Eqs. (24), (25) computed over the full duration of each trial. The error was computed separately for the longitudinal and lateral motions. In the figures, the black boxes indicate the manual control trials and the grey boxes indicate the haptic trials. The bottom and top edges of each box display the 25th and 75th percentile respectively. The vertical lines show the whiskers, and the horizontal lines represent the medians. As can be seen, overall haptic trials have lower values compared to the manual control trials. This suggests that the haptic feedback helped the pilot to accomplish the task with better performance compared to manual control.

Fig. 12 shows the boxplots of the control activity W with and without haptic aid. The figure shows the plots for the longitudinal and lateral motion separately (Figs. 12a,12b). Both figures show a significant decrease in pilot control activity when performing the task with haptic feedback (grey boxes) compared to manual control (black boxes).

Therefore, the expert pilot needed fewer control actions to control the helicopter with haptic aid, suggesting that the shared control system lowered pilot effort and did not generate conflicts with his actions.

According to these preliminary results, the proposed haptic shared control system was shown to help the expert pilot to perform the control task with better performance in terms of tracking error compared to manual control. Moreover, the task workload was found to be reduced with the help of the haptic feedback, as hypothesized. Overall, the proposed haptic shared control system did not disturb the expert pilot while controlling the helicopter dynamics and did not counteract his control actions.

V. Pilot-in-the-Loop Experiment

A final human-in-the-loop experiment was conducted to evaluate the effectiveness of the designed haptic shared control system on minimally-trained pilots. The experiment was performed with the experimental setup and control task described in Section III.

A. Participants

Thirteen minimally-trained participants participated in the experiment. All participants were trained in fixed-based simulators for performing a helicopter task. Specifically, six of them were trained in the MPI CyberMotion Simulator with no motion [28], in a previous work [29]. During the training, the participants learned how to hover the 6-DoF helicopter dynamics by performing increasingly-difficult tasks: hovering turns, vertical repositioning, vertical repositioning and heading, lateral/longitudinal hover, and complete hover. The participants were trained in two sessions, performed in two different days. In total each of them trained in the simulator with no motion for approximately 3 hours. None of them experienced real helicopter flight, and none of them had previous experience with haptic aids.

The remaining seven participants were trained in a different experiment, with a computer-based simulator (i.e. fixed-base) [30]. The experiment consisted of three different sessions: familiarization, training and evaluation. During the familiarization phase, participants performed the same increasingly difficult tasks as in the experiment described above. During the training phase, they were asked to perform the complete hover only. Finally, they performed the evaluation phase in the CyberMotion Simulator with no motion. The overall experiment (including all sessions) lasted approximately 3 hours. Moreover, none of the seven participants had ever experienced haptic feedback systems before.

B. Hypotheses

The proposed 2-DoF haptic shared control system was hypothesized to help minimally-trained helicopter pilots to fly and control the considered helicopter dynamics. As the haptic aid was designed to help pilots to track their intended trajectory, the tracking performance was expected to achieve better results (i.e, lower tracking error) with haptic aid compared to manual control. Moreover, lower control activity was hypothesized with the haptic feedback compared to

Table 3 Results of the ANOVA test on the tracking error for longitudinal and lateral motion separately. The value Fstat indicates the result of the F-statistic, the values DF1, DF2 indicate the degrees of freedom, and p is the p-value.

Longitudinal Motion	Fstat	DF1	DF2	p^a
HA vs NoAid	35.012	1	518	5.9633e-09
Lateral Motion				
HA vs NoAid	15.7	1	518	8.4629e-05

[a]For $p < 0.05$ the result is statistically significant.

the trials with manual control, as pilots were expected to adopt a different and less demanding control strategy.

C. Results

This section presents the results of the human-in-the-loop experiment conducted with thirteen minimally-trained participants to evaluate the proposed shared control system. The measures defined in Section III.E were computed per each participant and averaged overall the trials, as follows:

$$\begin{aligned} \bar{e}_x &= \frac{\sum_{i=1}^{N_T} e_x}{N_T} \\ \bar{e}_y &= \frac{\sum_{i=1}^{N_T} e_y}{N_T} \end{aligned} \tag{27}$$

where N_T is the total number of trials per each participant. The control activity W was averaged overall the trials similarly to Eq. (27). All measures were computed separately for longitudinal and lateral motion and then compared to evaluate the overall system.

A one-way analysis of variance (ANOVA) was carried out to investigate the statistical effect of the haptic aid (i.e. independent variable) on the considered dependent variables. To account for differences between participants capabilities, a linear mixed-effect/multilevel model was considered to fit data [31]. Then, the F-statistic was derived and the p-value was computed. The analysis was conducted separately for longitudinal and lateral motions.

1. Tracking performance

The tracking error was computed to measure pilot tracking performance. Boxplots are used to display the results. Fig. 13 shows the boxplots of the tracking errors achieved by all the participants overall the trials with and without haptic aid. Specifically, Fig. 13a shows the errors obtained during the longitudinal motion (i.e, first 40 s of each trial) and Fig. 13b shows the errors during the lateral motion (i.e, last 40 s of each trial). Both figures show that the medians of the grey boxes have lower values compared to the medians of the black boxes. This indicates that overall 50% of the participants performed the haptic trials with better performance compared to the trials with manual control.

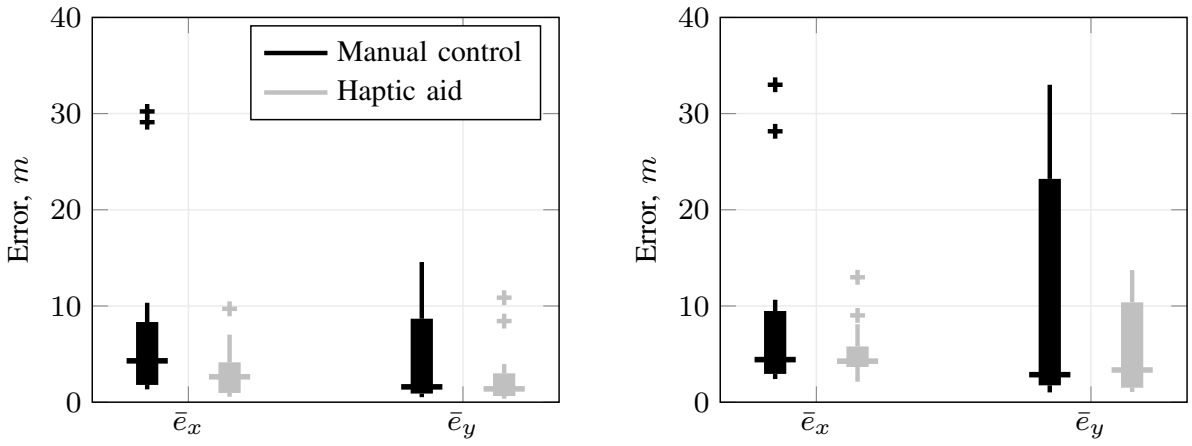

(a) Longitudinal motion. **(b) Lateral motion.**

Fig. 13 Experiment results: boxplots of the tracking error overall the trials of each participant

Table 4 Results of the ANOVA test conducted separately on the tracking errors $\bar{e}_x, \bar{e}_y$ for both longitudinal and lateral motion. The value Fstat indicates the result of the F-statistic, the values DF1, DF2 indicate the degrees of freedom, and p is the p-value.

Longitudinal Motion	Fstat	DF1	DF2	p^a
$\bar{e}_x$: HA vs NoAid	21.795	1	258	4.882e-06
$\bar{e}_y$: HA vs NoAid	15.924	1	258	8.5968e-05
Lateral Motion				
$\bar{e}_x$: HA vs NoAid	12.048	1	258	0.00060771
$\bar{e}_y$: HA vs NoAid	7.5763	1	258	0.0063338

[a]For $p < 0.05$ the result is statistically significant.

To validate the results, a statistical analysis was conducted. The analysis was carried out separately for longitudinal and lateral motion. Results of the ANOVA are shown in Table 3. The table shows the results in terms of F-statistic, degrees of freedom (DF1, DF2) and p-value. Specifically, DF1 indicates the indipendent variables, and DF2 indicates the number of data used in the analysis. The p-value is used to evaluate whether the statistical analysis produced significant results. Indeed, the results are considered highly significant when $p < 0.05$. As shown in the table, a significant difference was found between the tracking errors with and without haptic aid during the longitudinal motion: $F(1,518) = 35.012$ and $p << 0.001$. A main effect of the haptic system on the tracking performance was obtained also in the lateral motion, with $F(1,518) = 15.7$ and $p << 0.05$.

As the tracking errors were computed differently along the longitudinal and lateral directions (see Eqs. 24, 25), a further ANOVA analysis was conducted on longitudinal and lateral error $\bar{e}_x, \bar{e}_y$ separately within each motion condition, as shown by the boxplots in Fig. 13. The considered problem is described by a 2x2 linear mixed-effect/multilevel model with two dependent measures (lateral and longitudinal tracking errors) and two conditions (haptic trials and manual

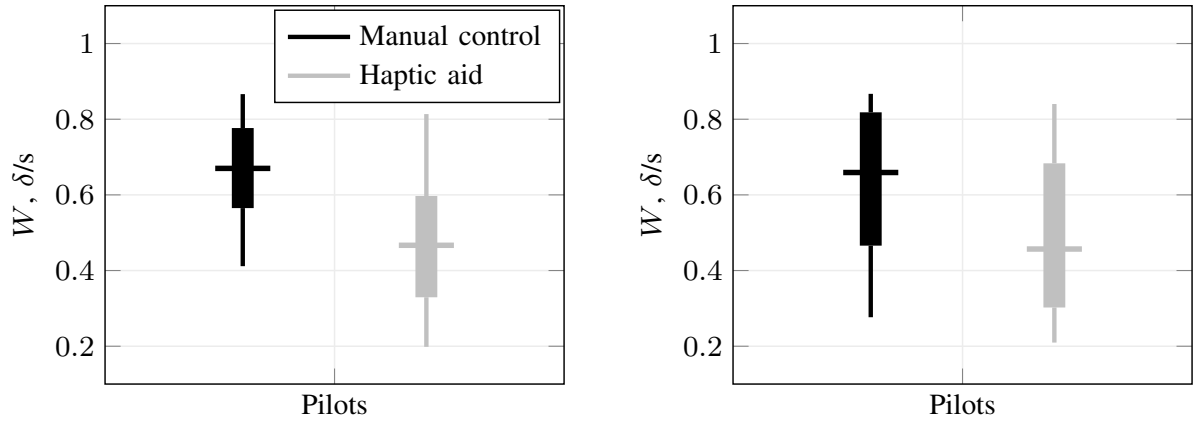

(a) Longitudinal motion. **(b) Lateral motion.**

Fig. 14 Experiment results: boxplots of the control activity overall the trials of each participant

Table 5 Results of the ANOVA test on the control activity for longitudinal and lateral motion separately. The value Fstat indicates the result of the F-statistic, the values DF1, DF2 indicate the degrees of freedom, and p is the p-value.

Longitudinal Motion	Fstat	DF1	DF2	p^a
HA vs NoAid	39.706	1	258	1.2684e-09
Lateral Motion				
HA vs NoAid	74.603	1	258	6.0969e-16

[a]For $p < 0.05$ the result is statistically significant.

control trials). Results are shown in Table 4. The test showed that the effect of the haptic aid on the tracking performance was statistically relevant for both errors during the longitudinal motion. Indeed, the results of the F-statistic showed the values: $F(1,258) = 21.795$, $p << 0.001$ for $\bar{e}_x$, and $F(1,258) = 15.924$, $p << 0.05$ for $\bar{e}_y$. Therefore, participants were facilitated by the haptic aid during the longitudinal motion, compared to manual control. The effectiveness of the haptic system resulted statistically significant on the longitudinal and lateral errors also during the lateral motion. The ANOVA test showed significant results: $F(1,258) = 12.048, p < 0.05$ for the longitudinal error, and $F(1,258) = 7.5763, p < 0.05$ for the lateral error (see Table 4).

2. Control activity

The amount of control activity was used to evaluate and compare pilot control strategy within each trial with and without haptic aid. Fig. 14 shows the boxplots of the control activity averaged overall the trials performed by each participant during both longitudinal and lateral motions. The black boxes indicate the manual control trials and the grey boxes indicate the haptic trials.

A one-way analysis of variance was conducted on the results obtained for the task workload, to investigate the

effectiveness of the haptic aid to reduce participants control effort. The results of the ANOVA test are presented in Table 5. A significant effect of the haptic system was obtained during both longitudinal and lateral motions. Specifically, results in the longitudinal motion showed a p-value much lower than the threshold value: $p << 0.05$. This suggests that, in the longitudinal motion, the haptic shared control reduced pilot control activity during the trials, as hypothesized. The same result is obtained for the lateral motion. Indeed, the ANOVA test showed a very small p-value (see Table 5).

VI. Discussion

Overall results of the experiment showed that the haptic feedback was effective to accomplish the task with lower tracking errors compared to manual control, during both longitudinal and lateral motions. Indeed, a significant difference between the two conditions was achieved with the statistical analysis. A slightly less significant statistic (but still having p-values $<< 0.05$) was obtained for the tracking error in the lateral motion, compared to the values obtained for the longitudinal motion. This indicates that participants behaved more similarly during the lateral motion with and without haptic aid, and that the force feedback enhanced only slightly their performance. This result may also suggest that the lateral motion was easier to be accomplished by the participants, compared to the longitudinal motion.

Further results analyzed the pilots control activity during each trial of the control task. Highly significant results were obtained between the two tested conditions. This indicates that the haptic aid was effective for the participants to reduce the control effort to accomplish the maneuver during the trials, as hypothesized. Therefore, overall pilots control strategy was less demanding during the trials performed with the haptic feedback switched on.

VII. Conclusion

In this paper, a 2 Degrees of Freedom (DoF) haptic shared control system was designed to help pilots to accomplish a lateral/longitudinal helicopter maneuver when no prior knowledge of the target trajectory can be assumed. Specifically, a Pilot Intent Estimator (PIE) was employed to infer pilot intended trajectory according to pilot actions on the control device. Then, a haptic aid was designed to track the estimated intended trajectory. To validate the proposed system, first, a preliminary test with an experienced helicopter pilot was carried out, to assess the PIE and to obtain a preliminary evaluation of the haptic feedback. Successively, a human-in-the-loop experiment was performed to evaluate the proposed shared control system. Thirteen minimally-trained participants participated in the experiment. The control task was to follow a target sphere, which performed two motions: longitudinal motion and lateral motion, with a hover condition in between. Each participant performed the task both with and without haptic aid.

Results from the preliminary test showed that the PIE correctly estimated the pilot intention to move along one specific direction, and the Trajectory Generator generated trajectories along the corresponding axes. The haptic feedback was shown to facilitate the expert pilot to accomplish the task, without interfering with his control actions. Indeed, the task workload of the expert pilot was reduced when the haptic aid was switched on.

Successively, the test campaign with thirteen participants proved the effectiveness of the haptic shared control system to help minimally-trained helicopter pilots to track the estimated intended trajectory. Participants in both longitudinal and lateral motions achieved significantly better performance in terms of tracking error, compared to manual control. Furthermore, the haptic feedback lowered participants control effort by reducing pilot control activity overall the trials.

These results show the effectiveness of the proposed 2-DoF haptic shared control system to help minimally-trained pilots to accomplish a lateral/longitudinal helicopter maneuver with no prior knowledge of the target trajectory. Specifically, the proposed system estimates according to pilot inputs, which is the most probable direction towards which the pilot intends to move, and generates intended trajectories along the corresponding axis. This allows the system to decouple pilot intention, as only one direction at a time is estimated as activated. The proposed algorithm may be extended to estimate also coupled maneuvers which are part of helicopters control, e.g. diagonal movements in a 2-DoF lateral/longitudinal scenario. A possible easy way to extend the algorithm may be to change the decider function for mode activation with mean values (or weighted values), such that both directions can be selected at each time instant. Generalization of the estimation algorithm to more complex maneuvers is currently under investigation by the authors.

References

[1] Wise, Hopkin, and Garland, *Handbook of aviation human factors*, 2nd ed., CRC Press Taylor & Francis Group, Boca Raton, FL, 2010, Chap. 8.

[2] Parasuraman, R., "Human-computer monitoring," *Human Factors*, Vol. 29, 1987, doi: https://doi.org/10.1177/001872088702900609, pp. 695–706.

[3] Parasuraman, R., and Mouloua, M., "Interaction of signal discriminability and task type in vigilance decrement," *Perception & Psychophysics*, Vol. 41(1), 1987, doi: https://doi.org/10.3758/BF03208208, pp. 17–22.

[4] Abbink, D., M, M., and Boer, E. R., "Haptic shared control: smoothly shifting control authority?" *Cognition, Technology and Work*, Vol. 14, No. 1, 2012, doi: https://doi.org/10.1007/s10111-011-0192-5, pp. 19–28.

[5] Alaimo, S. M. C., Pollini, L., Bresciani, J. P., and Bülthoff, H. H., "A comparison of direct and indirect haptic aiding for remotely piloted vehicles," *19th International Symposium in Robot and Human Interactive Communication*, 2010, doi: http://doi:10.1109/ROMAN.2010.5598647.

[6] Olivari, M., Nieuwenhuizen, F. M., Bülthoff, H. H., and Pollini, L., "Pilot adaptation to different classes of haptic aids in tracking tasks," *Journal of Guidance, Navigation and Dynamics*, Vol. 37, No. 6, 2014, doi: https://doi.org/10.2514/1.G000534, pp. 1741–1753.

[7] Mulder, M., Mulder, M., Van Passen, M. M., and Abbink, D. A., "Haptic gas pedal feedback," *Ergonomics*, Vol. 51, No. 11, 2008, doi: https://doi.org/10.1080/00140130802331583, pp. 1710–1720.

[8] Maimeri, M., Olivari, M., Bülthoff, H. H., and Pollini, L., "On effects of failures in haptic and automated pilot support systems," *AIAA SciTech Conference*, 2016, doi: https://doi.org/10.2514/6.2016-1181.

[9] D'Intino, G., Olivari, M., Geluardi, S., Venrooij, J., Innocenti, M., Bülthoff, H. H., and Pollini, L., "Evaluation of haptic support systems for training purposes in a tracking task," *IEEE International Conference on Systems, Man, and Cybernetics*, 2016, doi: http://doi:10.1109/SMC.2016.7844560.

[10] D'Intino, G., Olivari, M., Geluardi, S., Venrooij, J., Pollini, L., and Bülthoff, H. H., "Experimental evaluation of a haptic support system for learning a 2-DoF tracking task," *AIAA SciTech Conference*, 2017, doi: https://doi.org/10.2514/6.2017-1083.

[11] Bufalo, F., Olivari, M., Geluardi, S., Gerboni, C. A., Pollini, L., and Bülthoff, H. H., "Variable force-stiffness haptic feedback for learning a disturbance rejection task," *IEEE International Conference on Systems, Man, and Cybernetics*, 2017, doi: http://doi:10.1109/SMC.2017.8122829.

[12] Nieuwenhuizen, F. M., and Bülthoff, H. H., "Evaluation of haptic shared control and a highway-in-the-sky display for personal aerial vehicles," *AIAA SciTech Conference*, 2014, doi: https://arc.aiaa.org/doi/10.2514/6.2014-0808.

[13] Mulder, M., Abbink, D. A., and Boer, E. R., "The effect of haptic guidance on curve negotiation behavior of young, experienced drivers," *IEEE International Conference on Systems, Man, and Cybernetics*, 2008, doi: http://doi:10.1109/ICSMC.2008.4811377.

[14] Profumo, L., Pollini, L., and Abbink, D. A., "Direct and indirect haptic aiding for curve negotiation," *IEEE International Conference on Systems, Man, and Cybernetics*, 2013, doi: http://doi:10.1109/SMC.2013.318.

[15] Hoeckx, F., "Machine learning for haptic shared control: the effect of individualized haptic guidance paths for free-air teleoperation tasks," *TU Delft M.Sc. Thesis*, 2016.

[16] Krozel, J., and Andrisani, D., "Intent inference with path prediction," *Journal of Guidance, Control and Dynamics*, Vol. 29, No. 2, 2006, https://doi.org/10.2514/1.14348, pp. 225–236.

[17] D'Intino, G., Olivari, M., Geluardi, S., Fabbroni, D., Bülthoff, H. H., and Pollini, L., "A pilot intent estimator for haptic support systems in helicopter maneuvering tasks," *AIAA SciTech Conference*, 2018, doi: https://arc.aiaa.org/doi/10.2514/6.2018-0116.

[18] Mazor, E., Averbuch, A., Bar-Shalom, Y., and Dayan, J., "Interacting multiple model methods in target tracking: a survey," *IEEE Transaction on Aerospace and Electronic Systems*, Vol. 34, 1998, doi: http://doi:10.1109/7.640267, pp. 103–123.

[19] D'Intino, G., Arenella, A., Olivar, M., Bülthoff, H. H., and Pollini, L., "Experimental evaluation of a 2-DoF haptic shared control system based on pilot intent estimation," *IEEE International Conference on Systems, Man, and Cybernetics*, 2018, doi: http://doi:10.1109/SMC.2018.00546.

[20] Bar-Shalom, Y., Li, X. R., and Kirubarajan, T., *Estimation with application to tracking and navigation*, John Wiley & Sons, Inc, USA, 2001, Chap. 11.

[21] Geluardi, S., *Identification and augmentation of a civil light helicopter: transforming helicopters into Personal Aerial Vehicles*, Logos Verlag GmbH, Berlin, Germany, 2016, Chap. 2.

[22] McRuer, D. T., "Human pilot dynamics in compensatory systems: theory, models and experiments with controlled element and forcing function variations," *Air Force Flight Dynamics Laboratory*, 1965.

[23] Drop, M. F., *Control-theoretic models of feedforward in manual control*, CPI-Koninklijke Wöhrmann-Zutphen, 2016.

[24] Itoh, M., Flemisch, F., and Abbink, D. A., "A hierarchical framework to analyze shared control conflicts between human and machine," *IFAC PapersOnLine*, Vol. 49, No. 19, 2016, doi: https://doi.org/10.1016/j.ifacol.2016.10.468, pp. 96–101.

[25] Scholtens, W. M., "Reducing conflicts in haptic shared control during curve negotiation," *TU Delft M.Sc. Thesis*, 2018.

[26] Baskett, B. J., "Aeronautical design standard performance specification handling qualities requirements for military rotorcraft," *United States Army Aviation and Missile Command, Aviation Engineering Directorate*, 2000.

[27] Perfect, P., Jump, M., and White, M. D., "Handling qualities requirements for future personal aerial vehicles," *Journal of Guidance, Control, and Dynamics*, 2015, doi: https://doi.org/10.2514/1.G001073, pp. 1–13.

[28] Nieuwenhuizen, F. M., and Bülthoff, H. H., "The mpi cybermotion simulator: A novel research platform to investigate human control behavior," *JCSE*, Vol. 7, No. 2, 2013, doi: http://dx.doi.org/10.5626/JCSE.2013.7.2.122, pp. 122–131.

[29] Fabbroni, D., Bufalo, F., D'Intino, G., Geluardi, S., Gerboni, C. A., Olivari, M., and Bülthoff, H. H., "Transfer of training from fixed- and motion-base simulators to a light-weight helicopter," *74th AHS Annual Forum*, 2018.

[30] Scaramuzzino, P. F., D'Intino, G., Pavel, M. D., Pool, D. M., Stroosma, O., Mulder, M., and Bülthoff, H. H., "Effectiveness of a computer-based helicopter trainer for initial hover training," *44th European Rotorcraft Forum*, 2018.

[31] Pinheiro, J. C., and Douglas, M. B., "Unconstrained parametrizations for variance-covariance matrices," *Statistics and Computing*, Vol. 6, 1996, doi: https://doi.org/10.1007/BF00140873, pp. 289–296.